

Article

Association of Environmental Factors in the Taiwan Strait with Distributions and Habitat Characteristics of Three Swimming Crabs

Muhamad Naimullah ¹, Kuo-Wei Lan ^{1,2,*} , Cheng-Hsin Liao ¹, Po-Yuan Hsiao ¹, Yen-Rong Liang ¹ and Ting-Chen Chiu ¹

¹ Department of Environmental Biology Fisheries Science, National Taiwan Ocean University, 2 Pei-Ning Rd., Keelung 20224, Taiwan; 20831006@email.ntou.edu.tw (M.N.); chliao@mail.ntou.edu.tw (C.-H.L.); 00431016@mail.ntou.edu.tw (P.-Y.H.); 10831009@mail.ntou.edu.tw (Y.-R.L.); 10831011@mail.ntou.edu.tw (T.-C.C.)

² Center of Excellence for Oceans, National Taiwan Ocean University, 2 Pei-Ning Rd., Keelung 20224, Taiwan

* Correspondence: kwlan@mail.ntou.edu.tw; Tel.: +886-24622192 (ext. 5027)

Received: 18 June 2020; Accepted: 10 July 2020; Published: 11 July 2020



Abstract: Information regarding the oceanic environment is crucial for determining species distributions and their habitat preferences. However, in studies on crustaceans, especially swimming crabs, such information remains poorly utilized, and its effects on crab communities in the Taiwan Strait (TS) has not been well documented. The purpose of this study was to understand the relationship between the catch rates of three swimming crab species and environmental factors in the TS. We fitted generalized additive models (GAMs) to logbooks and voyage data recorder data from Taiwanese crab vessels (2011–2015), developed a species distribution model, and predicted catch rates for these three swimming crab species based on the GAM output. The chlorophyll-*a* (Chl-*a*) concentration was related to the high catch rates of *Chrybdis feriatius* and *Portunus sanguinolentus*, whereas bottom temperature (BT) was related to high catch rates of *Portunus pelagicus*. The variance percentages for each crab species indicated that high catch rates of *C. feriatius* and *P. sanguinolentus* occurred in a Chl-*a* concentration > 0.5 mg/m³, whereas *P. pelagicus* catch rates exhibited negative correlations with BTs > 25 °C. The model predicted high catch rates of *C. feriatius* in the north of the TS during autumn and winter, whereas *P. pelagicus* was observed to the south during summer and autumn. *P. sanguinolentus* was predicted to be widely distributed around the TS and distributed further to the northern area during autumn and winter. These findings revealed that each species responds to spatiotemporal environmental variations. Understanding the distributions and habitats of these three crabs is vital in fisheries resource management and conservation planning.

Keywords: crustacean; Portunidae; commercial crab; generalized additive models; habitat preference

1. Introduction

Understanding the spatial and temporal variability of key environmental variables within commercial fishing grounds is crucial in resource management to help identify species distributions and their habitat preferences. This information can be used to implement sustainable fisheries through methods, such as harvest strategy planning [1], ecosystem management [2,3], spatial management [4–6], and bycatch reduction [7]. Environmental variables, such as water temperature, salinity, water depth, and increased productivity, may be significant factors driving changes in population patterns [8,9], catch rates [10–12], reproductive and recruitment strategies [13–15], and spatiotemporal distribution [16,17].

The Taiwan Strait (TS) is located in the tropical to subtropical western Pacific region and is highly influenced by three currents: Kuroshio Branch Current, China Coastal Current, and South China Sea

(SCS) Current. These currents affect the marine environments and fishing grounds bordered by the East China Sea (ECS) and SCS to the south and north. On average, the TS is approximately 350 km, 180 km, and 60 m in length, width, and depth, respectively, and has a depth of more than 200 m in the southeastern portion [18–20]. Taiwan's crab species is diverse, with more than 250 species found in East Asia [21]. Trap fishing is commonly conducted in the coastal region of the northern TS on rocky substrates and trawl fishery is mostly conducted in the offshore waters of the southwestern and northern TS [22]. The crucifix crab (*Charybdis feriatus*), the blue swimming crab (*Portunus pelagicus*), and the three spot swimming crab (*Portunus sanguinolentus*) are three of the most crucial commercial species of crustaceans in Taiwan's coastal waters [23–25].

Crabs belong to a group of decapod crustaceans. Portunid crabs, collectively known as swimming crabs, are mostly found in the sandy-bottom areas of seas; furthermore, they are one of the crucial predator species in benthic habitats and are ecologically vital for the marine ecosystem [26]. Adult swimming crabs are known to travel long distances [23,27–29]. A distinctive characteristic of swimming crabs is that the legs of the last two segments of last pair make paddle-like movement, which results in swimming crabs having higher mobility than most other crustaceans. Because of the high mobility, determining the distribution of swimming crabs is a difficult modeling task. Environmental variables, such as sea surface temperature (SST) and bottom temperature (BT), currents, chlorophyll-*a* (Chl-*a*), and salinity, may influence the crab's distributions [8,9,30,31]. Additionally, the habitat preferences of the crab are mainly affected by the depth and sediment texture [23,32–34]. Furthermore, Chou et al. [35] revealed that the crustacean community compositions in southwestern waters of Taiwan were mainly determined using three factors, namely large-scale differences in water depth, characteristics of the bottom substrate, and topography, which influences the circulation of water.

C. feriatus is a portunid crab species widely distributed in the Indo-Pacific region usually found sublittorally on muddy and sandy bottoms, as well as on rocky and stony coasts, including coral reef flats, at depths of approximately 10–60 m [36]. *P. pelagicus* prefers sandy to sandy-muddy substrates in shallow waters, at a depth of 50 m, including areas near reefs and mangroves, as well as in seagrass and algal beds; it is commonly found in tropical and subtropical estuaries and nearshore habitats [37,38]. *P. pelagicus* is distributed from the eastern Mediterranean and East Africa in the Indian Ocean to Japan and Tahiti in the western and southern Pacific Ocean [37]. *P. sanguinolentus* is widely distributed in the Indo-Pacific region from the eastern coast of South Africa to waters around Hawaii [39,40]. *P. sanguinolentus* typically inhabits sandy oceanic habitats to a depth of 30 m [26].

Considerable progress has been achieved in species distribution modeling in marine environments [41]. To evaluate environmental feature parameters affecting the behavior, range, and biology of the species, the concerned species' distribution prediction models are useful when adequate location data are available, independent from bias, and accessible [42]. For crabs, applications of species distribution modeling includes predicting appropriate habitat distribution [30,34], monitoring crab intrusion [43], and predicting fishing grounds [13,44], which are a new trend in predicting crab fishery locations. The effects of these factors on crab communities in the waters of Taiwan have not been sufficiently documented. The purpose of this study was to understand the seasonal variation in catch rates of three common swimming crab species and its association with environmental factors in the TS. The species distribution modeling of *P. sanguinolentus*, *P. pelagicus*, and *C. feriatus* was developed using the generalized additive models (GAM). Furthermore, using the observed catch rates and the selected environmental factors, we predicted the catch rates and compared the predicted accuracy for the three crabs in TS. Based on this information, sustainable crab fisheries can be implemented in the future through improved fisheries management and conservation planning in TS.

2. Materials and Methods

2.1. Swimming Crab Fishery Data

Data on *P. sanguinolentus*, *P. pelagicus*, and *C. feriatus* from 2011 to 2016 were collected from the voyage data recorder and logbooks of 170 Taiwanese crab vessels (5–200 metric tons) in the TS. The fishing data consisted of daily fishing positions for 0.1° spatial grids including latitude and longitude, fishing date, soaking time, total catch (kg), and crab species. Swimming crabs were collected using circular crab traps with frozen mackerel as bait in the center of the pot [39].

2.2. Marine Environmental Data

Daily SST, sea surface height (SSH), BT, and sea surface salinity (SSS) marine environmental data were extracted from the Hybrid Coordinate Ocean Model and a Navy Coupled Ocean Data Assimilation. The SST model (ETOPO5) had a spatial resolution of 9 km (apdrc.soest.hawaii.edu). Bathymetry data were downloaded from the Asia Pacific Data Research Center (apdrc.soest.hawaii.edu). The SSH can be used to infer oceanic features, such as current dynamics, fronts, eddies, and convergences [45]. Monthly Chl-*a* data were downloaded from the NASA Aqua satellite (oceancolor.gsfc.nasa.gov), which features a sensor to detect the concentration of Chl-*a* in the world's oceans, among other applications. The level 3 data map image Chl-*a* data have a monthly temporal resolution and 4.6-km (at the equator) spatial resolution. The environmental data were then calculated monthly on a spatial grid of 0.1° to fit the fishery data using Interface Descriptive Language version (IDL) 7.0. The environmental data were tested for intercorrelations before running the statistical models to determine the correlation coefficients among the variables. The test for intercorrelations among all environmental variable explained low correlation coefficients ($r^2 < 0.25$).

2.3. Spatial and Temporal Statistical Models of Swimming Crab Catch Rates

Monthly observed catch rates were calculated using the cumulative weight of each crab species caught from all fishing vessels for a month divided by the cumulative soaking time for all set lines in that month to adjust for fishing effort. Monthly observed catch rates were calculated for individual 0.1° grids across the study region by using the following expression:

$$\text{Observed catch rate}_{ij} = \frac{\Sigma \text{Catch for all vessels (kg)}_{ij}}{\Sigma \text{Soaking time for all vessels (hour)}_{ij}}, \quad (1)$$

where i represents the latitude, and j represents the longitude of each 0.1° spatial grid. We divided the observed catch rates of each species into five groups on the basis of cumulative frequency.

We created a spatial distribution of catch percentages map of *P. sanguinolentus*, *P. pelagicus*, and *C. feriatus* caught in the TS from 2011 to 2016 between 20.5°N and 29°N and between 118°E and 125.5°E using Quantum GIS version 3.6 [46]. We constructed a seasonal mean catch rate map of the three species using IDL from 2011 to 2016 in the TS. Maps were generated for each of the four seasons: spring (March–May), summer (June–August), autumn (September–November), and winter (December–February).

To more thoroughly understand the association of observed catch rates for each crab species with the environmental factors, the longitudinal and latitudinal gravitational centers of the observed catch rates (G) were estimated using monthly longitudinal and latitudinal locations of crab vessels (L) and monthly observed catch rates [47,48]:

$$G_{ij} = \frac{\Sigma L_{ij} \times \text{observed catch rate}_{ij}}{\Sigma \text{observed catch rate}_{ij}} \quad (2)$$

We plotted the monthly mean trends of G presented in relation to the monthly mean values of environmental data of *C. feriatius*, *P. pelagicus*, and *P. sanguinolentus* from 2011 to 2016 in the TS.

We examined the effects of environmental variability on observed catch rates using GAMs [49]. The GAMs were created using R version 3.6 [50] through the “mgcv” package GAM function. The observed catch rate was the response variable, and environmental factors (SST, BT, SSS, SSH, Chl-*a*, and depth) were the predictor variables. The GAM is summarized as follows:

$$\log(\text{catch rates}) = s(\text{SST}) + s(\text{BT}) + s(\text{SSH}) + s(\text{SSS}) + s(\text{Chl-}a) + s(\text{Depth}) \quad (3)$$

In Equation (3), $s(xn)$ is a spline smoothing function for each model covariate xn . The model with the optimal conformation was selected using a stepwise procedure that was based on the lowest value of the Akaike’s information criterion (AIC), and the p -value of the final set of variables was lower than 0.05. We used the coefficient of determination (r^2) to evaluate the precision of the model prediction [30].

2.4. Predictions of Swimming Crab Catch Rates

The output from the selected GAM environmental factors was used to predict the catch rates of three commercial swimming crabs in the TS from 2011 to 2015. We mapped the seasonal mean of the predicted observed catch rates overlaid with the most explained variance percentages of the environmental variable by GAM of three swimming crabs in the TS. The selected GAMs were based on the data from 2011 to 2015, and the environmental data of 2016 were used to predict the catch rates of three crabs. Furthermore, we tested the prediction accuracy of high catch rates (>60% of cumulative frequency) by comparing the observed and predicted catch rates of fishery data in 2016 for the year and seasonal changes by using cumulative frequency. The root mean square error (RMSE) were used to measure how far the prediction was from the observed output, which is formulated as follows:

$$\text{RMSE} = \sqrt{\frac{\sum_{i=1}^n [\log(\text{observed high catch rates}_i) - \log(\text{predicted high catch rates}_i)]^2}{n}} \quad (4)$$

3. Results

3.1. Spatial and Temporal Distribution of Three Crab Species in the TS

The spatial distribution revealed that *P. sanguinolentus* was widely distributed from south to north in the TS (Figure 1), whereas *C. feriatius* and *P. pelagicus* were mostly distributed in southern and northern TS, respectively. The seasonal spatial distributions of observed catch rates illustrated that each species was distributed in different areas during different seasons (Figure 2). During winter, *C. feriatius* was mainly distributed in the northern areas of TS, moved southwest during spring, and could be found in northern areas during the summer and autumn (Figure 2a–d). The distribution of *P. pelagicus* was more concentrated near the southern coast of Taiwan in the TS during winter and spring, and it could also be found near southern and northern Taiwan during summer and autumn (Figure 2e–h). The spatial distribution of *P. sanguinolentus* was widespread in the TS in all seasons, and its distribution was further northeast in spring, summer, and autumn (Figure 2i–l).

The time series of latitudinal and longitudinal G of the catch rates (Figure 3a–b) and monthly mean environmental parameters in catch positions (Figure 3c–h) for each species exhibited different trends in the TS. The monthly latitudinal and longitudinal G for *C. feriatius* exhibited stable seasonal variations, whereas *P. pelagicus* moved from the southern (>23.25°N) and western (<120.25°E) areas with an increase in the SST, BT, SSH, Chl-*a*, and depth and decrease in the SSS during summer and autumn. For *P. sanguinolentus*, when SST, SSH, and depth increased and BT, SSS, and Chl-*a* decreased during spring and summer, the latitudinal and longitudinal G moved to northern and eastern areas of the TS. Furthermore, in 2012–2013, the latitudinal and longitudinal G of *P. sanguinolentus* moved further into northern (>25.75°N) and eastern (>122.75°E) areas during spring and summer.

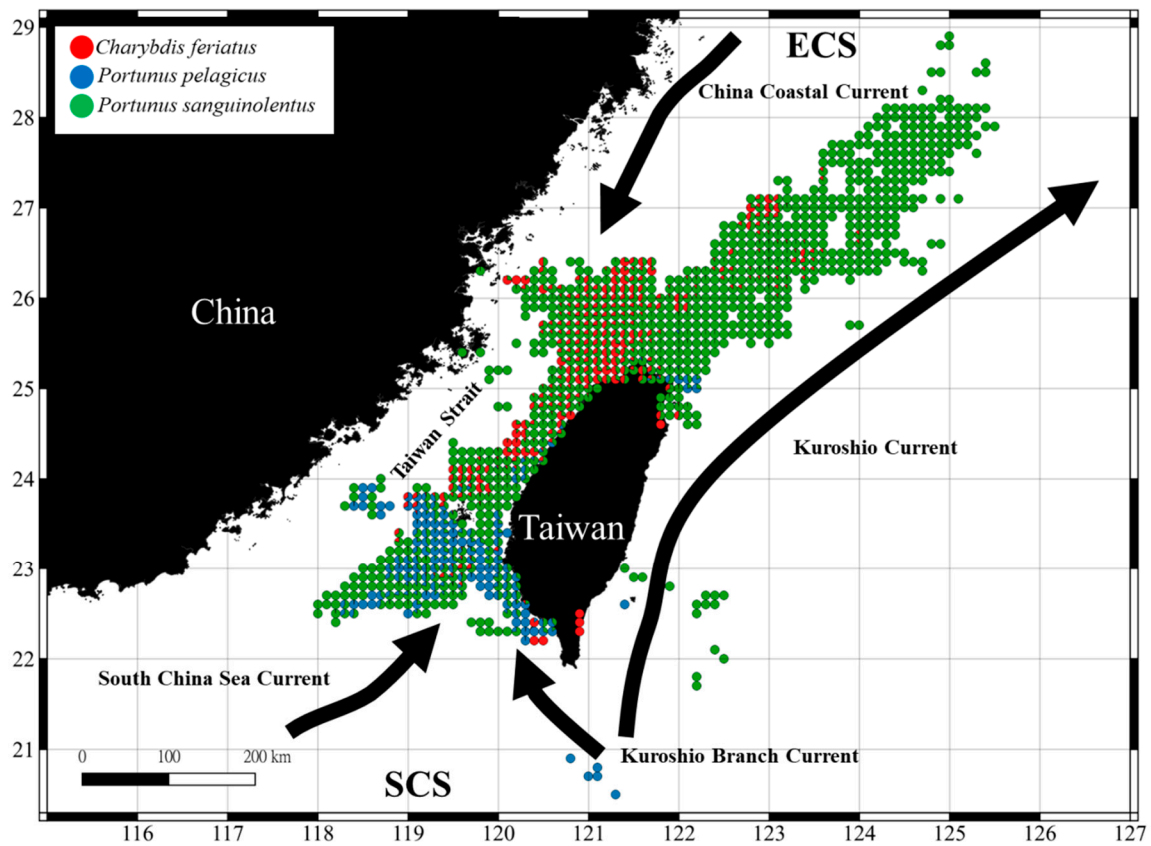


Figure 1. Spatial distributions of catch of *C. feriatius*, *P. pelagicus*, and *P. sanguinolentus* caught using crab traps from 2011 to 2016 in the Taiwan Strait (TS).

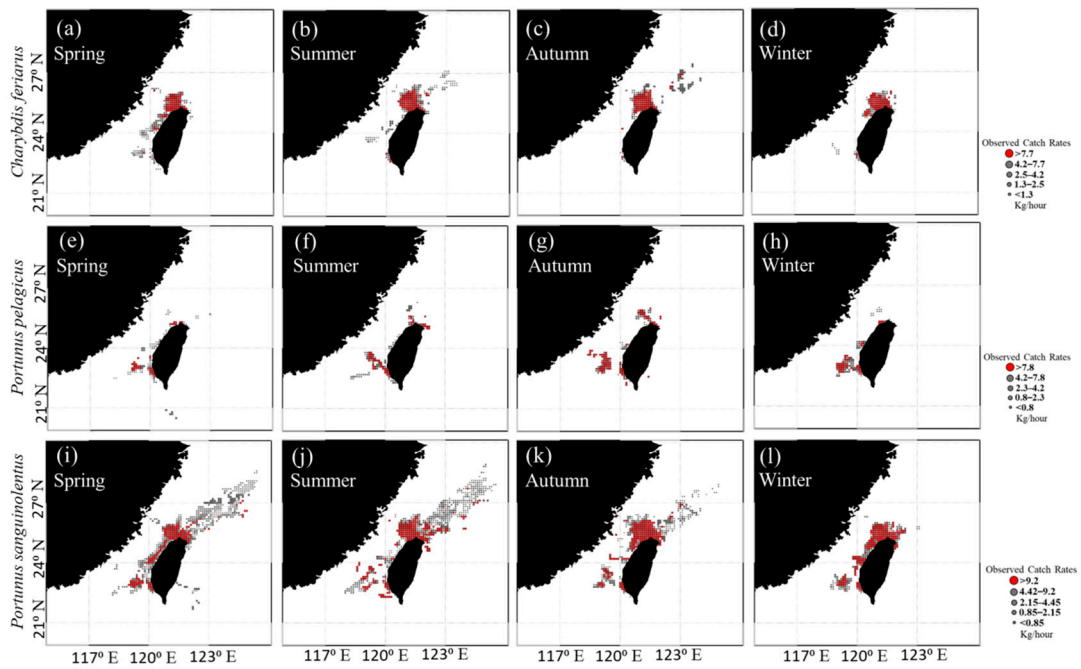


Figure 2. Seasonal mean observed catch rates of *C. feriatius* (a–d), *P. pelagicus* (e–h), and *P. sanguinolentus* (i–l).

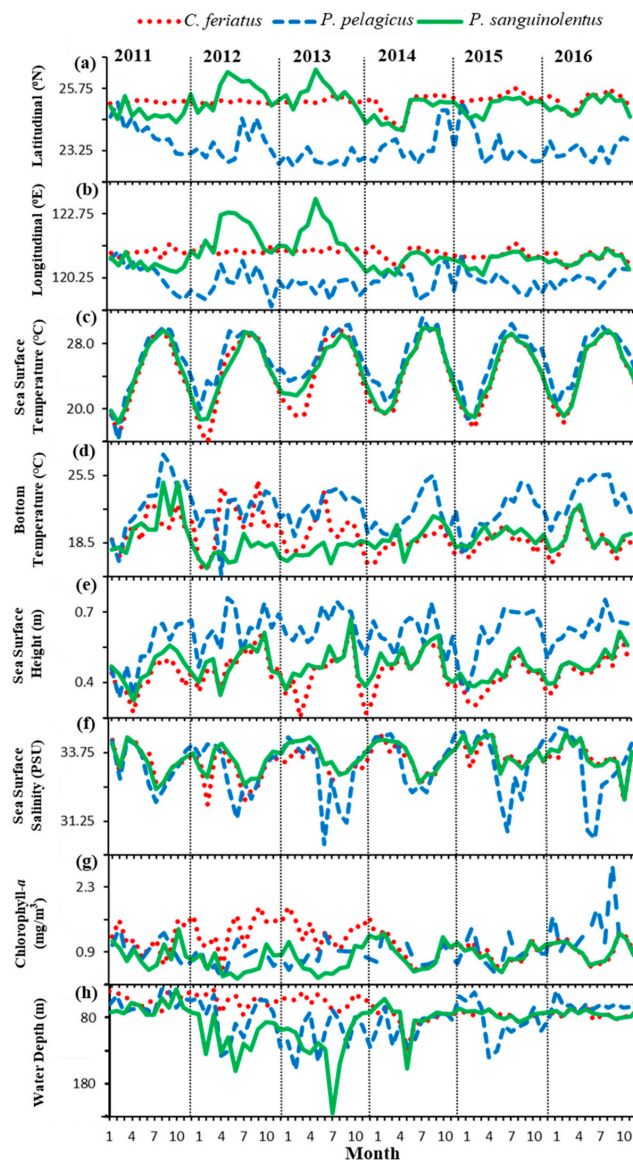


Figure 3. Monthly mean trends of (a) latitudinal (Lat.) and (b) longitudinal (Lon.) gravitational centers of observed catch rates (G) of *C. feriatius*, *P. pelagicus*, and *P. sanguinolentus*, presented in relation to the monthly mean values of (c) sea surface temperature (SST); (d) bottom temperature (BT); (e) sea surface height (SSH); (f) sea surface salinity (SSS); (g) chlorophylla- a (Chl- a); and (h) water depth (Depth) in the TS.

3.2. Environmental Effect on Swimming Crab Catch Rates

The total variances derived using the GAMs for *C. feriatius*, *P. pelagicus*, and *P. sanguinolentus* were 38.1%, 24.0%, and 21.7% in 2011–2015, respectively (Table 1). Statistically, all the variables examined for the three crab species in the TS were highly substantial predictors ($p < 0.01$). The addition of environmental variables led to the increased variance, which was attributed to decreased AIC. Chl- a explained the most significant amount of variance for *C. feriatius*, followed by the depth and SST, and SSS explained the lowest amount (Table 1). Similar to *C. feriatius*, Chl- a , depth, and SST also explained the largest amount of variance for *P. sanguinolentus*, but SSH explained the least for this species (Table 1). By contrast, for *P. pelagicus*, BT explained the largest amount of variance, followed by the depth and SSS, and SST explained the smallest amount of variance for this species (Table 1).

Table 1. Explained one variable model variances (EV, %) of observed catch rates in the generalized additive models with environmental variables sequentially added (first to last) for *C. feriatius*, *P. pelagicus*, and *P. sanguinolentus* in the TS (all $p < 0.01$). The determination coefficient (r^2) represented the predictive performance of model predictability.

Variable	<i>C. feriatius</i>		<i>P. pelagicus</i>		<i>P. sanguinolentus</i>	
	EV, %	AIC	EV, %	AIC	EV, %	AIC
+s (SST)	11.0	5983.908	1.80	3698.498	2.55	18392.500
+s (BT)	2.33	5950.341	7.27	3653.093	2.32	18284.730
+s (SSH)	3.64	5838.423	3.09	3631.735	0.68	18221.980
+s (SSS)	2.20	5708.007	5.34	3562.240	2.15	17966.830
+s (Chl- <i>a</i>)	22.6	5403.713	2.45	3551.349	12.1	17371.340
+s (Depth)	14.7	5340.132	6.55	3509.710	6.13	17326.040
Total variance explained (%)	38.1		24.0		21.7	
r^2	0.34		0.18		0.19	

The seasonal mean observed catch rates overlaid on selected environmental factors based on the largest model-explained variance percentages of each crab species illustrate that both *C. feriatius* and *P. sanguinolentus* mostly aggregated in waters with a Chl-*a* value of > 0.5 mg/m³, whereas, *P. pelagicus* catch rates had negative correlations with BTs > 25 °C (Figure 4). The GAM results suggested that the catch rates of *C. feriatius* (Figure 5a–f) had positive correlations with SSTs > 20 °C and Chl-*a* > 0.5 mg/m³ but had negative correlations with BTs > 15 °C, SSHs > 0.6 m, SSSs > 33 PSU, and depths > 100 m. For *P. pelagicus*, the catch rates exhibited positive correlation with SSTs > 20 °C, and SSHs > 0.5 m, but exhibited negative correlations with BTs > 25 °C, SSSs > 33 PSU, Chl-*a* > 1.0 mg/m³, and depths > 100 m (Figure 5g–l). Moreover, for *P. sanguinolentus*, the GAM results suggested that the catch rates had a positive correlation with SSTs > 20 °C, SSHs > 0.4 m, Chl-*a* > 0.5 mg/m³, and depths > 200 m but had negative correlations with BTs > 15 °C and SSSs > 33 PSU (Figure 5m–r).

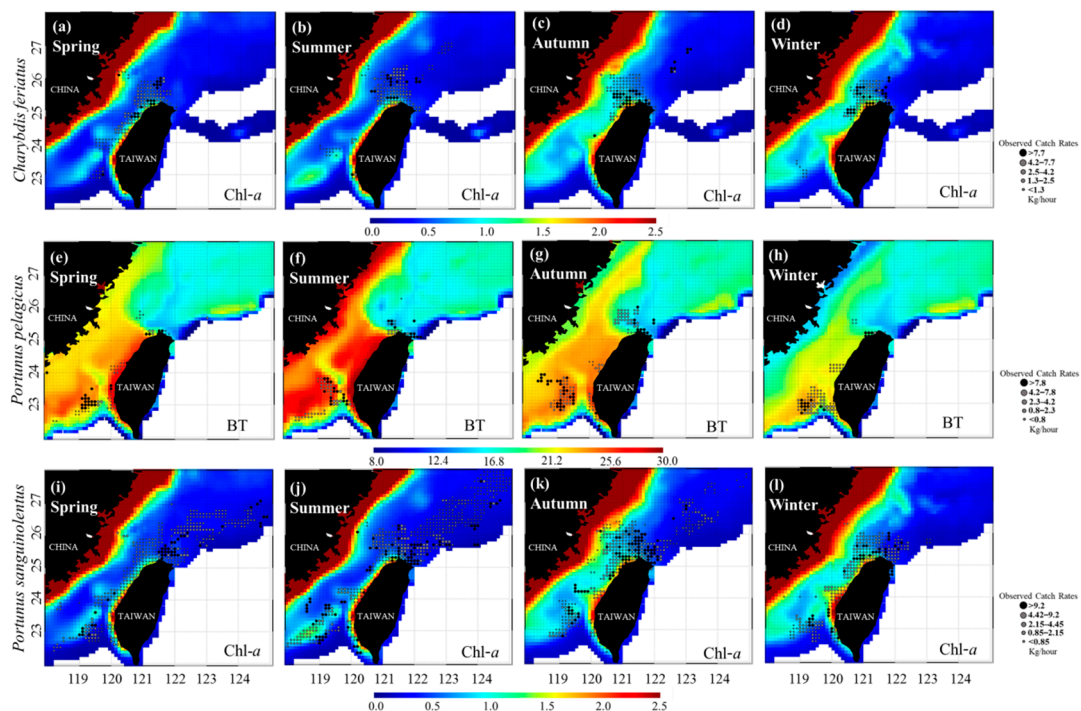


Figure 4. Seasonal mean observed catch rates of *C. feriatius*, *P. pelagicus*, and *P. sanguinolentus* during spring, summer, autumn, and winter, 2011–2016, overlaid with Chl-*a* (a–d), (i–l) and BT (e–h).

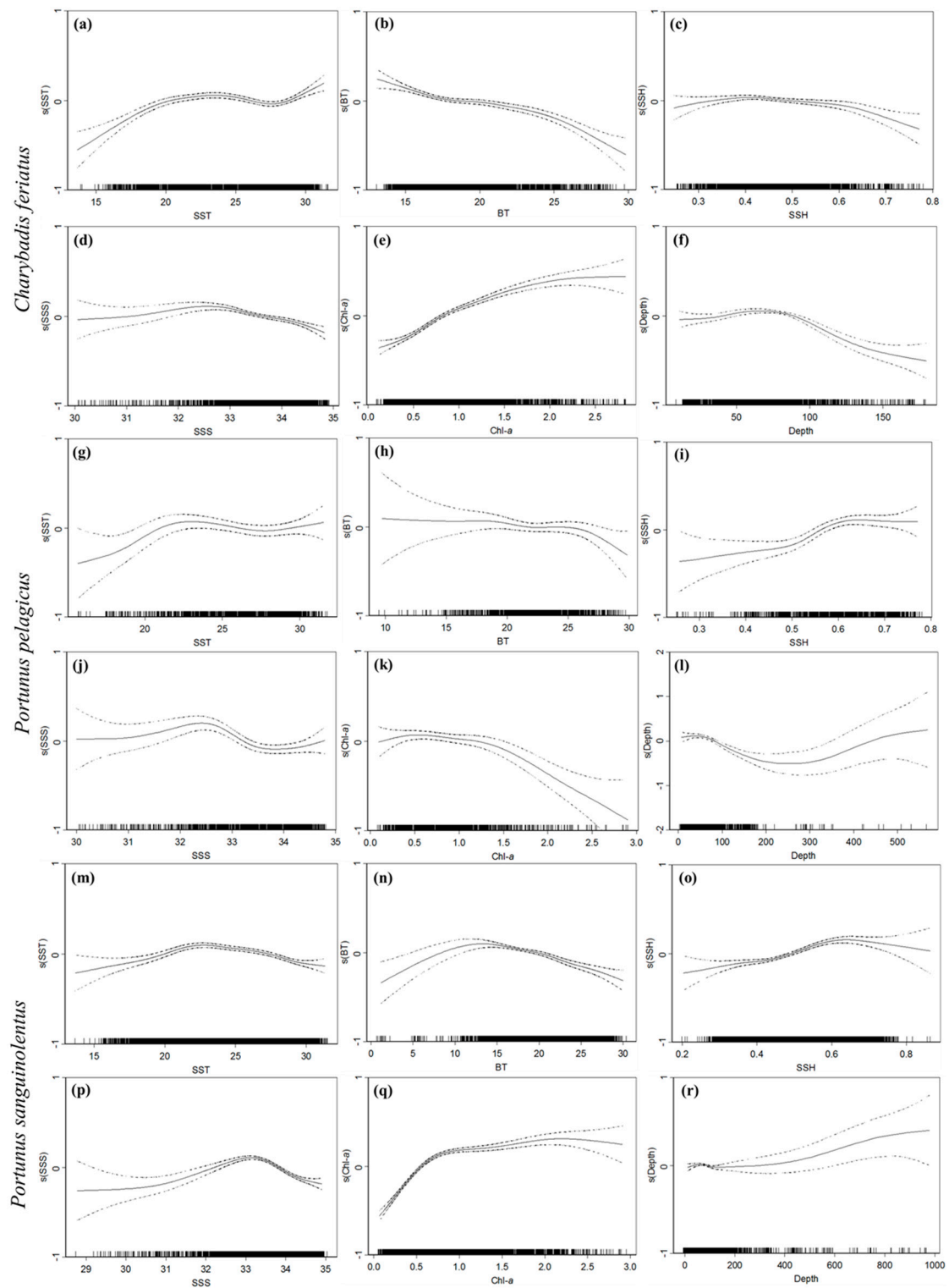


Figure 5. Effects of environmental factors on catch rates of three commercial swimming crabs in the TS: (a–f) *C. feriatatus*, (g–l) *P. pelagicus*, and (m–r) *P. sanguinolentus*. The black dotted and solid lines in figures a–r denote the fitted generalized additive model function and 95% confidence interval, respectively. The relative density of data points is indicated by the rug plot on the x-axis, and the y-axis shows the results of smoothing the fitted values; furthermore, $s(x_n)$ represents a spline smoothing function for each model covariate x_n .

3.3. Predicted Spatial Distributions of the Three Crab Species

Figure 6 presents images of a seasonal mean observed catch rate map overlaid on predicted catch rates for *C. feriatus*, *P. pelagicus*, and *P. sanguinolentus* in the TS. High catch rates of *C. feriatus* were predicted in the north TS between 25°N and 26°N, and these catch rates decreased during spring and summer (Figure 6a,b). A high catch rate of *C. feriatus* was predicted in the southwest of the region, including in coastal water of mainland China, during autumn and winter (Figure 6c,d). The predicted catch rates of *C. feriatus* extended to 25°N–26°N and 122°E–123°E in the TS during summer and autumn. For *P. pelagicus*, a high catch rate was predicted further to the south of the TS between 22°N and 24°N, and some fishing locations extended to the northeast at 25°N–26°N (Figure 6e–h). The catch distribution of *P. pelagicus* was mostly from the northern part of the SCS to the TS and then decreased during spring (Figure 6e). The seasonal predicted catch rates of *P. sanguinolentus* were widely distributed around the TS, and fishing positions also extended southwest to a region that includes coastal water of mainland China before being extended further to the northern area during autumn and winter (Figure 6k,l). Finally, the catch rates of *P. sanguinolentus* decreased during spring and summer in the TS.

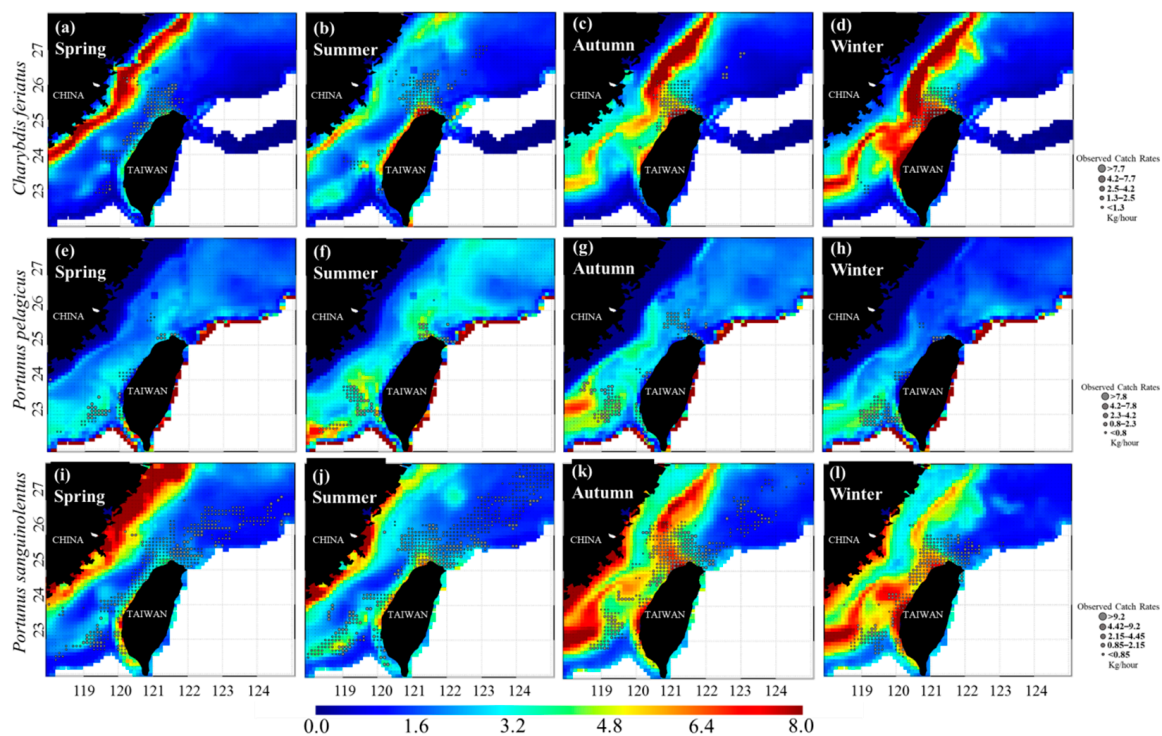


Figure 6. Seasonal mean of observed catch rates of *C. feriatus* (a–d), *P. pelagicus* (e–h), and *P. sanguinolentus* (i–l) overlaid with catch rates predicted by selected generalized additive models (GAMs) in 2011–2015.

The prediction accuracy and RMSE exhibited seasonal variations for *C. feriatus*, *P. pelagicus*, and *P. sanguinolentus* in 2016 (Table 2). *C. feriatus* exhibited a high accuracy percentage in autumn (67.23%) and winter (55.95%) but a low percentage in spring (26.42%) and winter (22.05%), whereas *P. pelagicus* exhibited a high accuracy percentage during the three seasons, winter (77.27%), spring (76.19%), and summer (64.0%) but low in autumn (37.5%). However, *P. sanguinolentus* showed only a high percentage in autumn (83.87%) and a low accuracy percentage in winter (46.88%), spring (58.78%), and summer (24.24%). The RMSE for *C. feriatus*, *P. pelagicus*, and *P. sanguinolentus* were in the range between 0.37 to 0.84.

Table 2. Numbers (>60%) of observed (O) and predicted (P) high catch rates of *C. feriatus*, *P. pelagicus*, and *P. sanguinolentus* in the TS in 2016. The RMSE represented the test error metric of cumulative frequency results.

Season	<i>C. feriatus</i>			<i>P. pelagicus</i>			<i>P. sanguinolentus</i>		
	O	P	RMSE	O	P	RMSE	O	P	RMSE
Spring	53	14	0.48	42	32	0.49	131	77	0.54
Summer	127	28	0.47	25	16	0.78	66	16	0.60
Autumn	177	119	0.37	16	6	0.84	186	156	0.38
Winter	84	47	0.44	22	17	0.45	160	75	0.52
Year	438	205	0.43	75	39	0.64	488	261	0.49

4. Discussion

4.1. Portunid Crab Distribution in the TS

The results of this study demonstrated that the observed catch rates of *P. sanguinolentus* were widely spread from the south to the north of the TS, whereas the observed catch rates of *P. pelagicus* were separated into two main areas in the south and north of the TS. However, the observed catch rates of *C. feriatus* were mostly distributed in the northern TS. Shaohua [51] reported that Portunidae is a dominant crab species from the central and northern TS and generally higher in number in offshore waters and lower in eastern waters. Ye et al. [52] and Ye [53] have revealed that *C. feriatus* is the dominant crab species in the north of TS, and *P. sanguinolentus*, and *P. pelagicus* are dominant species around the Taiwan Bank. The results in the present study also postulated that the three important commercial swimming crab species react to different types of habitats caused by environmental factors.

Figure 7 indicates that *C. feriatus* was mainly distributed near northern Taiwan in winter and extended to the southwest during spring and could be found to the north during summer and autumn. Furthermore, a high predicted catch rate of *C. feriatus* was observed southwestward of TS during autumn and winter, including coastal mainland China (Figure 6c,d). Huang [54] discovered that the catch rate of *C. feriatus* in the southern part of the ECS was the highest during winter and lowest during summer, and the primary breeding seasons were spring and summer. Huang [54] also suggested that winter is the optimal season for *C. feriatus* fishing based on the distribution of their numbers, their biological characteristics, and the fishing production status. Some studies have shown that swimming crabs that inhabit marine embayment often do not leave these marine environments to spawn [55,56]. Furthermore, compared with other swimming crab species, *C. feriatus* can breed continually, and the broodstock is available year-round [57]. Thus, we suggested that the distribution of *C. feriatus* mainly in northern TS could be due to a particular factor and the preferred seasons for fishing this species being autumn and winter.

P. pelagicus was more concentrated on the southern coast of the TS and highly catch rates in the northern TS during summer and autumn (Figure 7). High *P. pelagicus* concentrations were observed at the south of TS during summer and autumn, and the concentration decreased during winter and spring. The highest seasonal catch rates of *P. pelagicus* were also recorded during summer in the Arabian Sea [38,58] and between December and May along the coast of Tanzania [59]. Similar to *C. feriatus*, *P. pelagicus* also appears to have a particular preferred distribution and habitat in the TS. Studies have revealed that female *P. pelagicus* spawn in estuaries. Such individuals then emigrate into coastal marine water and release their eggs [55]. Large numbers of *P. pelagicus* were obtained in a sandy-muddy site in South TS influenced by freshwater runoff from the Kaoping River [23]. Furthermore, juvenile crabs inhabit shallow waters and migrate to deeper water when they grow larger [60]. These observations indicate that *P. pelagicus* has seasonal variation because they prefer habitats near an estuarine area with sand-mud substrates and brackish waters during the juvenile stages and then migrate deeper in the TS.

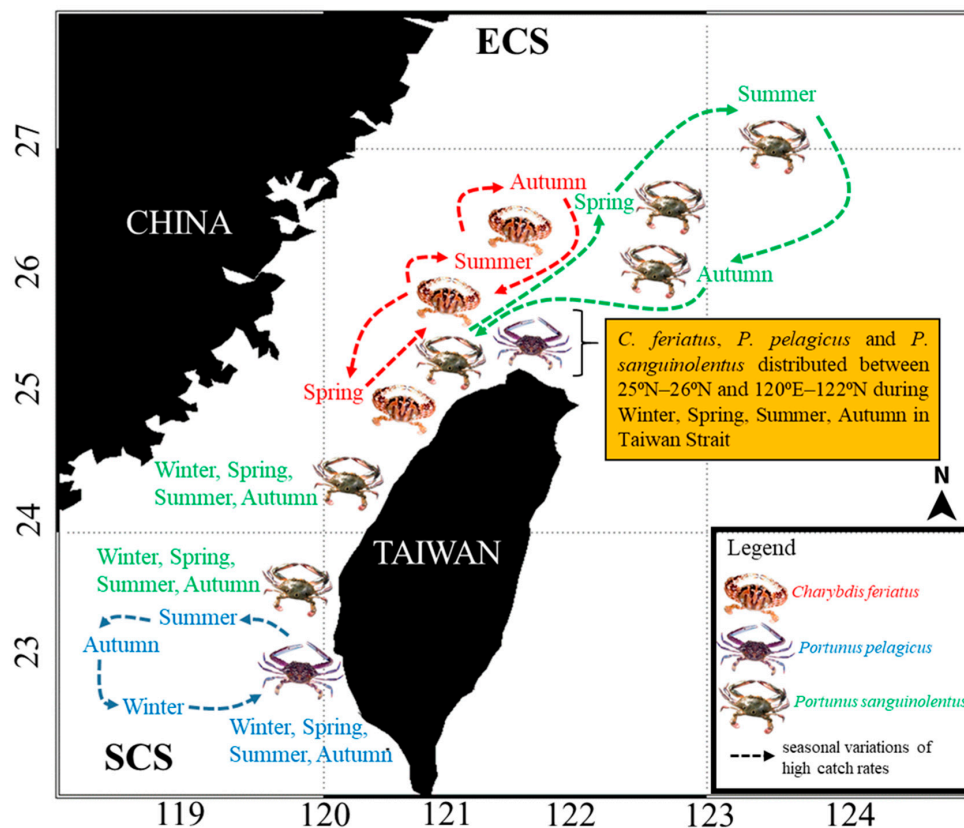


Figure 7. Illustration of the seasonal spatial distribution variations in high catch rates of *C. feriatius*, *P. pelagicus*, and *P. sanguinolentus* in the TS.

For *P. sanguinolentus*, the spatial distribution was widespread in the TS for all seasons, and the distribution were further northeast during spring, summer, and autumn (Figure 7). The seasonal predicted catch rates of *P. sanguinolentus* was also widely distributed around the TS and spread southwestward of the strait, including coastal mainland China, and then extended further to the northern area during autumn and winter. Samuel and Soundarapandian [61] mentioned that the peak seasons of *P. sanguinolentus* catch rates were from May to August and from October to December along the southeast coast of India. Huang et al. [62] revealed that the catch rates of *P. sanguinolentus* considerably decreased during spring along the coastal regions of China. *P. sanguinolentus* distribution and habitat seems more widespread in TS probably because these species can tolerate a wide range of environmental factors. Furthermore, sea currents may also be a primary factor the wide distribution of *P. sanguinolentus* in TS. According to Rasheed and Mustaqim [40], most of *P. sanguinolentus* larvae hatch as zoea drift in the water current before inhabiting benthic habits and grow into a juvenile crab. Throughout the year, in TS, strong Kuroshio Branch Current and SCS Current during the summer and autumn may affect the movement of *P. sanguinolentus* in the northern area. *P. sanguinolentus* typically inhabit the sandy and muddy bottom in the shallow area [26,63], whereas adult and berried females often migrate to deeper waters for spawning [24,64], which results in widespread distribution of this species.

4.2. Effects of Ocean Environmental Variables on the Swimming Crabs

Understanding the relationships between environmental effects and fundamental processes related to variation in catch rates is crucial. All three crab species exhibited different distribution trends in the TS based on seasons and habitats. The Chl-*a* concentration explained the largest variance in GAM for *C. feriatius* and *P. sanguinolentus*. In previous habitat studies, environmental factors, such as organic matter, temperature, sediment size, and salinity, have been considered to

influence variations in the diversity and distribution of crab species in both time and space [11,65]. Furthermore, Signa et al. [66] determined that the density of the swimming crab *Polybius henslowii* is strongly related to the concentration of Chl-*a*, suggesting more accumulation in locations with higher production. Moreover, the highest catch rates of *C. smithii* near Arabian sea coasts and pelagic red crab *Pleuroncodes planipes* along the coastal area of Baja California were recorded in upwelling systems [67,68]. In South-East Queensland, Australia, spanner crab *Ranina ranina* catch rates were the highest during the seasonal favorable upwelling in spring due to increased feeding during the mating season [8]. Essential fishing ground was mostly related to the upwelling area that consisted of a high Chl-*a* concentration and low SST that carried large amounts of nutrients from the bottom layer to the surface layer of the ocean [69] and is a crucial factor affecting the diet of *C. feriatius* and *P. sanguinolentus* in TS.

For *P. pelagicus*, BT explained considerable variance and had negative correlations with BTs >25 °C in the TS. Studies have revealed that the water temperature is a factor that controls the ovarian development and spawning of *P. pelagicus* [10,24,58]. Moreover, Qari and Aljarari [58] mentioned that temperature is a critical environmental parameter that plays a role in limiting the distribution and activity of *P. pelagicus* in the Red Sea. Furthermore, in Chesapeake Bay and South-East Queensland, when the water temperature was low, the catch rates of *Callinectes sapidus* and *R. ranina* increased considerably [8,70]. Andrade et al. [12] determined that in continental shelf waters off the Southeast Region of Brazil, neither SST nor BT had significant effects on swimming crabs, whereas, the spatial distributions of *C. bimaculata*, *C. japonica*, and *P. trituberculatus* in Haizhou Bay, China, were mostly affected by BT [30]. These differences could be because of the regions where the studies were conducted. The TS is located in a temperate region, with large variations in temperature throughout the year. The temperature not only affects the distribution of crabs but is also a critical factor in their reproduction, growth, and life stage.

Salinity appears to be one of the most critical environmental factors affecting the reproductive cycle, with higher salinities being favorable for breeding for portunid crabs [71]. Moreover, bottom salinity significantly influenced the distribution of *C. bimaculata*, indicating that the preferred salinity range was 29–31 in Haizhou Bay [30]. *P. sanguinolentus* females mostly inhabit deeper waters and prefer higher salinity compared with male crabs [72]. Salinity differences also affected the catch rates and habitat of *C. danae* and *C. ornatus*, which are commonly caught in areas with low salinity and estuary regions off the northeast coast of Brazil [73]. However, salinity explained among the lowest variance in GAM of the three important commercial swimming crabs in the TS. Jan et al. [74] discovered that bottom and surface sea salinity in TS varied. The bottom area recorded higher salinity throughout the year. The fishery data in the present study were collected from a crab trap, and the sub-surface salinity should be investigated in a future study.

The depth is a crucial environmental factor shaping the community structure of swimming crabs in bottom environments, and changes in the structure of benthic communities may be related to the depth incline [11,33]. The composition of benthic crustacean communities near southwestern Taiwan was influenced by the water depth [35]. The species composition and distribution of crabs in the southern ECS were mostly related to the water depth and were maximum at a depth of 100–120 m, followed by 80–100 m [52]. Moreover, at the northern continental shelf in the SCS, the largest aggregation of crab species was mainly distributed at depths of 10–60 m with a peak in depths near 10 m [25]. Our GAM finding indicated that higher catch rates of *C. feriatius*, *P. pelagicus*, and *P. sanguinolentus* were observed at depths of approximately 100 m in the TS. Huang [54] also revealed that *C. feriatius* was mainly distributed in areas where the depth was less than 80 m in the southern part of ECS.

In the present study, *P. sanguinolentus* was distributed in the water of various depths around the north and southwest parts of the TS. Hsueh and Hung [24] suggested that the breeding of *P. sanguinolentus* is associated with high temperature and deeper waters areas near southern TS. *P. sanguinolentus* juveniles were often found in high concentrations in estuaries and inshore waters; adults were more abundant in deep waters; and females were abundant at depths of 40–80 m [22,72,75].

P. sanguinolentus females were abundant at a depth of 80 m, whereas males prefer depths of 40–60 m in the north of TS [39]. Thus, we conclude that the distribution of *P. sanguinolentus* in the TS moves toward the north of Taiwan and into deeper waters during spring, summer, and autumn, which could be because mature crabs breed during these seasons and require deeper and warmer areas.

Notably, swimming crabs adapt to their habitat and distribution of space and time. Because the TS is located in the East Asian monsoon region, wind direction changes with the seasons causes a different current that affects the marine environment and species [76]. The availability of light as a source of energy for photosynthesis, mineral nutrients, and temperature, which influence their metabolic rate, play a crucial role in regulating Chl-*a* in the oceans [77]. In addition, the high salinity and temperature with low nutrients from the warm SCS current and Kuroshio Branch Current flows in summertime and the strong northeastern winds push the fresh, cold, nutrient-rich China Coastal Current southward along the western part of the TS [78]. This causes a complex bottom topography, and the several current systems in TS result in changes in essential variables, such as Chl-*a* and BT, which affect these crabs.

The spatial and temporal variables in GAM analyses is critical because GAM is used to determine whether changes in catch rates are related to these environmental variables or some other spatial and temporal variables that are unaccounted for. However, most higher amount of variance in GAM analyses were attributed to the spatial and temporal variables. Lower variance was observed for environmental variables [8,30,31,48]. The environmental variables change over time and positions and their effect should be considered in fishery regulations [9,45]. Furthermore, the geographic information probably quite well known by fishers and fishery managers, and our seasonal catch rate distributions of three crabs in Figures 1–4 also could support the similar results. Our results suggested that models of catch rates that incorporate relevant environmental variables can be used to infer possible responses in the distribution of swimming crabs. Climate variability leads to changes in the fishing location. Further studies should investigate the annual variations to explore future changes in distributions for the swimming crabs.

5. Conclusions

In summary, our results confirmed that the distributions of *C. feriatus*, *P. pelagicus*, and *P. sanguinolentus* were related to spatiotemporal environmental variations in the TS. The Chl-*a* concentration accounted for significant catch rates for *C. feriatus* and *P. sanguinolentus*. BT accounted for the high catch rates for *P. pelagicus*. The high catch rates of *C. feriatus* and *P. sanguinolentus* occurred at a Chl-*a* concentration $> 0.5 \text{ mg/m}^3$, whereas *P. pelagicus* catch rates had negative correlations with BTs $> 25^\circ\text{C}$. The model predicted high catch rates of *C. feriatus* in the north during autumn and winter, whereas *P. pelagicus* was observed further to the south during summer and autumn in TS. The predicted catch rate of *P. sanguinolentus* was widely distributed around the TS for all seasons and distributed further to the northern area during autumn and winter. Based on this information, sustainable crab fisheries can be implemented in the future through harvest strategy planning, ecosystem management, spatiotemporal management, and bycatch reduction. We suggest that other environmental factors, such as bottom salinity, sediment type, and organic matter content, should be added in future modeling to improve predictions. This is because the natural habitat of crabs is often at the bottom of the sea, and a species' habitat considerably affects its catch rates. Moreover, recording the carapace size and sex of swimming crabs during the study period is essential for future studies to conduct a more comprehensive investigation of the influence of environmental factors on crab habitats and distributions.

Author Contributions: All authors have read and agree to the published version of the manuscript. Conceptualization, K.-W.L.; methodology, K.-W.L. and M.N.; software, P.-Y.H. and Y.-R.L.; formal analysis, P.-Y.H. and T.-C.C.; resources, C.-H.L.; data curation, M.N. and C.-H.L.; writing—original draft preparation, M.N.; writing—review and editing, M.N. and K.-W.L.; supervision, K.-W.L.

Funding: This research received no external funding.

Acknowledgments: This study was financially supported by the Council of Agriculture (107AS-11.2.1-FA-F1 and 108AS-9.2.1-FA-F1) and the National Science Council (MOST 107-2611-M-019-017 and MOST 108-2611-M-019-007).

We are grateful to the Taiwan Ocean Conservation and Fisheries Sustainability Foundation for providing data from Taiwanese crab vessels. This manuscript was edited by Wallace Academic Editing.

Conflicts of Interest: The authors declare no conflict of interest.

References

1. Kruse, G.H.; Zheng, J.; Stram, D.L. Recovery of the Bristol Bay stock of red king crabs under a rebuilding plan. *ICES J. Mar. Sci.* **2010**, *67*, 1866–1874. [[CrossRef](#)]
2. Szuwalski, C.S.; Punt, A.E. Fisheries management for regime-based ecosystems: A management strategy evaluation for the snow crab fishery in the eastern Bering Sea. *ICES J. Mar. Sci.* **2013**, *70*, 955–967. [[CrossRef](#)]
3. Kunsook, C.; Gajasen, N.; Paphavasit, N. A stock assessment of the blue swimming crab *Portunus pelagicus* (Linnaeus, 1758) for sustainable management in Kung Krabaen Bay, Gulf of Thailand. *Trop. Life Sci. Res.* **2014**, *25*, 41.
4. Gutiérrez, N.L.; Masello, A.; Uscudun, G.; Defeo, O. Spatial distribution patterns in biomass and population structure of the deep sea red crab *Chaceon notialis* in the Southwestern Atlantic Ocean. *Fish. Res.* **2011**, *110*, 59–66. [[CrossRef](#)]
5. Frid, A.; McGreer, M.; Stevenson, A. Rapid recovery of Dungeness crab within spatial fishery closures declared under indigenous law in British Columbia. *Glob. Ecol. Conserv.* **2016**, *6*, 48–57. [[CrossRef](#)]
6. Masello, A.; Defeo, O. The deep-sea red crab *Chaceon notialis* (Geryonidae) in the southwestern Atlantic Ocean: Spatial patterns and long-term effects of fishing. *Fish. Res.* **2016**, *183*, 254–262. [[CrossRef](#)]
7. Morris, A.S.; Wilson, S.M.; Dever, E.F.; Chambers, R.M. A test of bycatch reduction devices on commercial crab pots in a tidal marsh creek in Virginia. *Estuar. Coasts* **2011**, *34*, 386–390. [[CrossRef](#)]
8. Spencer, D.M.; Brown, I.W.; Doubell, M.J.; Brown, C.J.; Redondo Rodriguez, A.; Lee, S.Y.; Zhang, H.; Lemckert, C.J. Bottom boundary layer cooling and wind-driven upwelling enhance the catchability of spanner crab (*Ranina ranina*) in South-East Queensland, Australia. *Fish. Oceanogr.* **2019**, *28*, 317–326. [[CrossRef](#)]
9. Spencer, D.M.; Doubell, M.J.; Brown, I.W.; Rodriguez, A.R.; Lee, S.Y.; Lemckert, C.J. Environmental indices for spanner crab (*Ranina ranina*) catch rates depend on regional oceanographic features. *Estuar. Coast. Shelf Sci.* **2019**, *228*, 106–361. [[CrossRef](#)]
10. De Lestang, S.; Bellchambers, L.M.; Caputi, N.; Thomson, A.W.; Pember, M.B.; Johnston, D.J.; Harris, D.C. Stock–recruitment–environment relationship in a *Portunus pelagicus* fishery in Western Australia. In *Biology and Management of Exploited Crab Populations under Climate Change*; Kruse, G.H., Eckert, G.L., Foy, R.J., Lipcius, R.N., Sainte-Marie, B., Stram, D.L., Woodby, D., Eds.; Alaska Sea Grant, University of Alaska Fairbanks: Fairbanks, AK, USA, 2010; pp. 443–460. [[CrossRef](#)]
11. Lima, P.A.; Andrade, L.S.; Alencar, C.E.R.D.; Pereira, R.T.; Teixeira, G.M.; Fransozo, A. Two species of swimming crabs of the genus *Achelous* (Crustacea, Brachyura): Environmental requirements determining the niche. *Hydrobiologia* **2014**, *727*, 197–207. [[CrossRef](#)]
12. Andrade, L.S.; Frameschi, I.F.; Costa, R.C.; Castilho, A.L.; Fransozo, A. The assemblage composition and structure of swimming crabs (Portunoidea) in continental shelf waters of southeastern Brazil. *Cont. Shelf Res.* **2015**, *94*, 8–16. [[CrossRef](#)]
13. Johnston, D.; Harris, D.; Caputi, N.; Thomson, A. Decline of a blue swimmer crab (*Portunus pelagicus*) fishery in Western Australia—History, contributing factors and future management strategy. *Fish. Res.* **2011**, *109*, 119–130. [[CrossRef](#)]
14. Szuwalski, C.; Punt, A.E. Regime shifts and recruitment dynamics of snow crab, *Chionoecetes opilio*, in the eastern Bering Sea. *Fish. Oceanogr.* **2013**, *22*, 345–354. [[CrossRef](#)]
15. Andrade, L.S.; Frameschi, I.F.; Castilho, A.L.; Costa, R.C.; Fransozo, A. Can the pattern of juvenile recruitment and population structure of the speckled swimming crab *Arenaeus cribrarius* (Decapoda: Brachyura) be determined by geographical variations? *Mar. Ecol.* **2015**, *36*, 950–958. [[CrossRef](#)]
16. De Anda-Montañez, J.A.; Martínez-Aguilar, S.; Balart, E.F.; Zenteno-Savín, T.; Méndez-Rodríguez, L.; Amador-Silva, E.; Figueroa-Rodríguez, M. Spatio-temporal distribution and abundance patterns of red crab *Pleuroncodes planipes* related to ocean temperature from the Pacific coast of the Baja California Peninsula. *Fish. Sci.* **2016**, *82*, 1–15. [[CrossRef](#)]

17. Thorson, J.T. Measuring the impact of oceanographic indices on species distribution shifts: The spatially varying effect of cold-pool extent in the eastern Bering Sea. *Limnol. Oceanogr.* **2019**, *64*, 2632–2645. [[CrossRef](#)]
18. Liang, W.D.; Tang, T.Y.; Yang, Y.J.; Ko, M.T.; Chuang, W.S. Upper-ocean currents around Taiwan. *Deep Sea Res. Part II Top. Stud. Oceanogr.* **2003**, *50*, 1085–1105. [[CrossRef](#)]
19. Huh, C.A.; Lin, H.L.; Lin, S.; Huang, Y.W. Modern accumulation rates and a budget of sediment off the Gaoping (Kaoping) River, SW Taiwan: A tidal and flood dominated depositional environment around a submarine canyon. *J. Mar. Syst.* **2009**, *76*, 405–416. [[CrossRef](#)]
20. Huh, C.A.; Chen, W.; Hsu, F.H.; Su, C.C.; Chiu, J.K.; Lin, S.; Liu, C.S.; Huang, B.J. Modern (<100 years) sedimentation in the Taiwan Strait: Rates and source-to-sink pathways elucidated from radionuclides and particle size distribution. *Cont. Shelf Res.* **2011**, *31*, 47–63.
21. Ng, P.K.; Wang, C.H.; Ho, P.H.; Shih, H.T. *An annotated checklist of brachyuran crabs from Taiwan (Crustacea: Decapoda)*; National Taiwan Museum: Taipei, Taiwan, 2001; Volume 11.
22. Hsu, C.C.; Chang, H.C.; Liu, H.C. Sex-variant morphometrics of the swimming Crab, *Portunus sanguinolentus* (Herbst), from the. *J. Fish. Soc. Taiwan* **2000**, *27*, 175–185.
23. Hsueh, P.W.; Ng, P.K.; Hung, H.T. Brachyuran crab assemblages in subtidal soft-bottom habitats of Taiwan. *J. Fish. Soc. Taiwan* **2006**, *33*, 28–294.
24. Hsueh, P.W.; Hung, H.T. Temporal and spatial reproductive patterns of subtidal brachyuran crabs in coastal waters of Taiwan. *Crustaceana* **2009**, 449–465.
25. Huang, Z.R. Species composition and quantitative distribution of crabs in the northern continental shelf of South China Sea. *J. Dalian Fish. Univ.* **2009**, *6*, 14.
26. Sumpton, W.D.; Smith, G.S.; Potter, M.A. Notes on the biology of the portunid crabs, *Portunus sanguinolentus* (Herbst) in subtropical Queensland waters. *Aust. J. Mar. Freshw. Res.* **1989**, *40*, 711–717. [[CrossRef](#)]
27. Potter, M.A.; Sumpton, W.D.; Smith, G.S. Movement, fishing sector impact and factors affecting the recapture rate of tagged crabs, *Portunus pelagicus* (L.) in Moreton Bay, Queensland. *Aust. J. Mar. Freshw. Res.* **1991**, *42*, 751–760. [[CrossRef](#)]
28. Ikhwanuddin, M.; Nurfaseha, A.H.; Abol-Munafi, A.B.; Shabdin, M.L. Movement patterns of blue swimming crab, *Portunus pelagicus* in the Sarawak coastal water, South China Sea. *J. Sustain. Sci. Manag.* **2012**, *7*, 1–8.
29. Carr, S.D.; Tankersley, R.A.; Hench, J.L.; Forward, R.B., Jr.; Luettich, R.A., Jr. Movement patterns and trajectories of ovigerous blue crabs *Callinectes sapidus* during the spawning migration. *Estuar. Coast. Shelf Sci.* **2004**, *60*, 567–579. [[CrossRef](#)]
30. Luan, J.; Zhang, C.; Xu, B.; Xue, Y.; Ren, Y. Modelling the spatial distribution of three Portunidae crabs in Haizhou Bay, China. *PLoS ONE* **2018**, *13*, e0207457. [[CrossRef](#)]
31. Spencer, D.M.; Brown, I.W.; Doubell, M.J.; McGarvey, R.; Lee, S.Y.; Lemckert, C.J. Bottom Currents Affect Spanner Crab Catch Rates in Southern Queensland, Australia. *Mar. Coast. Fish.* **2019**, *11*, 248–257. [[CrossRef](#)]
32. Furlan, M.; Castilho, A.L.; Fernandes-Goes, L.C.; Fransozo, V.; Bertini, G.; Costa, R.C. Effect of environmental factors on the abundance of decapod crustaceans from soft bottoms off southeastern Brazil. *An. Da Acad. Bras. De Ciências* **2013**, *85*, 1345–1356. [[CrossRef](#)]
33. Bertini, G.; Fransozo, A. Bathymetric distribution of brachyuran crab (Crustacea, Decapoda) communities on coastal soft bottoms off southeastern Brazil. *Mar. Ecol. Prog. Ser.* **2004**, *279*, 193–200. [[CrossRef](#)]
34. De la Barra, P.; Svendsen, G.; Romero, M.A.; Avaca, M.S.; Narvarte, M. Predicting the distribution of a portunid crab in Patagonian coastal waters. *Mar. Ecol. Prog. Ser.* **2020**, *638*, 95–105. [[CrossRef](#)]
35. Chou, W.R.; Lai, S.H.; Fang, L.S. Benthic crustacean communities in waters of southwestern Taiwan and their relationships to environmental characteristics. *Acta Zool. Taiwanica* **1999**, *10*, 25–33.
36. Abelló, P.; Hispano, C. The capture of the Indo-Pacific crab *Charybdis feriata* (Linnaeus, 1758) (Brachyura: Portunidae) in the Mediterranean Sea. *Aquat. Invasions* **2006**, *1*, 13–16. [[CrossRef](#)]
37. Edgar, G.J. Predator-prey interactions in seagrass beds. II. Distribution and diet of the blue manna crab *Portunus pelagicus* Linnaeus at Cliff Head, Western Australia. *J. Exp. Mar. Biol. Ecol.* **1990**, *139*, 23–32. [[CrossRef](#)]
38. Hosseini, M.; Vazirzade, A.; Parsa, Y.; Mansori, A. Sex ratio, size distribution and seasonal abundance of blue swimming crab, *Portunus pelagicus* (Linnaeus, 1758) in Persian Gulf Coasts, Iran. *World Appl. Sci. J.* **2012**, *17*, 919–925.
39. Lee, H.H.; Hsu, C.C. Population biology of the swimming crab *Portunus sanguinolentus* in the waters off northern Taiwan. *J. Crustac. Biol.* **2003**, *23*, 691–699. [[CrossRef](#)]

40. Rasheed, S.; Mustaqim, J. Size at sexual maturity, breeding season and fecundity of three-spot swimming crab *Portunus sanguinolentus* (Herbst, 1783) (Decapoda, Brachyura, Portunidae) occurring in the coastal waters of Karachi, Pakistan. *Fish. Res.* **2010**, *103*, 56–62. [[CrossRef](#)]
41. Monk, J. How long should we ignore imperfect detection of species in the marine environment when modelling their distribution? *Fish. Fish.* **2014**, *15*, 352–358. [[CrossRef](#)]
42. Dell, J.; Wilcox, C.; Hobday, A.J. Estimation of yellowfin tuna (*Thunnus albacares*) habitat in waters adjacent to Australia's East Coast: Making the most of commercial catch data. *Fish. Oceanogr.* **2011**, *20*, 383–396. [[CrossRef](#)]
43. Compton, T.J.; Leathwick, J.R.; Inglis, G.J. Thermogeography predicts the potential global range of the invasive European green crab (*Carcinus maenas*). *Divers. Distrib.* **2010**, *16*, 243–255. [[CrossRef](#)]
44. Shanks, A.; Roegner, G.C.; Miller, J. Using megalopae abundance to predict future commercial catches of Dungeness crabs (*Cancer magister*) in Oregon. *Rep. Calif. Coop. Ocean. Fish. Investig.* **2010**, *51*, 106–118.
45. Lan, K.W.; Shimada, T.; Lee, M.A.; Su, N.J.; Chang, Y. Using remote-sensing environmental and fishery data to map potential yellowfin tuna habitats in the tropical Pacific Ocean. *Remote Sens.* **2017**, *9*, 444. [[CrossRef](#)]
46. QGIS Development Team. QGIS 3.6 Noosa. 2019. Available online: <https://qgis.org/en/site> (accessed on 30 September 2019).
47. Lehodey, P.; Bertignac, M.; Hampton, J.; Lewis, A.; Picaut, J. El Niño Southern Oscillation and tuna in the western Pacific. *Nature* **1997**, *389*, 715–718. [[CrossRef](#)]
48. Lan, K.W.; Evans, K.; Lee, M.A. Effects of climate variability on the distribution and fishing conditions of yellowfin tuna (*Thunnus albacares*) in the western Indian Ocean. *Clim. Chang.* **2013**, *119*, 63–77. [[CrossRef](#)]
49. Wood, S.N. *Generalized Additive Models: An Introduction with R*; Chapman and Hall/CRC: Boca Raton, FL, USA, 2017.
50. R Development Core Team. *R: A Language and Environment for Statistical Computing*; R Foundation for Statistical Computing: Vienna, Austria, 2018; Available online: <http://www.R-project.org> (accessed on 30 September 2019).
51. Shaohua, F. Crabs from central and northern Taiwan Strait. *J. Oceanogr. Taiwan Strait* **1991**, *4*.
52. Ye, S.Z.; Zhang, Z.L.; Ye, Q.T. Species composition and characteristics of crab distribution in south East China Sea. *J. Oceanogr. Taiwan Strait* **2006**, *25*, 387.
53. Ye, S.Z. Species composition and distribution characteristics of crab on Minnan-Taiwan bank fishing grounds. *Mar. T fisheries* **2004**, *4*, 1.
54. Huang, P.-M. The amount distribution and biological characteristics of *Charybdis feriatus* in the southern part of East China Sea. *J. Fujian Fish.* **2006**, *1*, 4.
55. Potter, I.C.; de Lestang, S. Blue swimmer crab *Portunus pelagicus* in Leschenault Estuary and Koombana Bay, south-western Australia. *J. R. Soc. West. Aust.* **2000**, *83*, 443–458.
56. Polity, I.A.; Muhamad, J.H.; Long, S.M.; Bolong, A.M.A. Fecundity of blue swimming crab, *Portunus pelagicus* Linnaeus, 1758 from Sematan fishing district, Sarawak coastal water of South China Sea. *Borneo J. Resour. Sci. Technol.* **2011**, *1*, 46–51. [[CrossRef](#)]
57. Baylon, J.; Suzuki, H. Effects of changes in salinity and temperature on survival and development of larvae and juveniles of the crucifix crab *Charybdis feriatus* (Crustacea: Decapoda: Portunidae). *Aquaculture* **2007**, *269*, 390–401. [[CrossRef](#)]
58. Qari, S.; Aljarari, R. The effect of season and acclimation on the heat and cold tolerance of the Red Sea Crab, *Portunus pelagicus*. *Life Sci. J.* **2014**, *11*, 145–148.
59. Chande, A.I.; Mgaya, Y.D. The fishery of *Portunus pelagicus* and species diversity of portunid crabs along the Coast of Dar es Salaam, Tanzania. *West. Indian Ocean J. Mar. Sci.* **2003**, *2*, 75–84.
60. Hisam, F.; Hajisamae, S.; Ikhwanuddin, M.; Pradit, S. Distribution pattern and habitat shifts during ontogeny of the blue swimming crab, *Portunus pelagicus* (Linnaeus, 1758) (Brachyura, Portunidae). *Crustaceana* **2020**, *93*, 17–32. [[CrossRef](#)]
61. Samuel, N.J.; Soundarapandian, P. Fishery Potential of Commercially Important Crab *Portunus sanguinolentus* (Herbst) along Parangipettai Coast, South East Coast of India. *Int. J. Anim. Veter. Adv.* **2009**, *1*, 99–104.
62. Huang, J.R.; Brown, C.L.; Yang, T.B. Spatio-temporal patterns of crab fisheries in the main bays of Guangdong Province, China. *Iran. J. Fish. Sci.* **2011**, *10*, 425–436.

63. Carpenter, K.E.; Krupp, F.; Jones, D.A.; Zajonz, U. FAO species identification field guide for fishery purpose. In *The Living Marine Resources of Kuwait, Eastern Saudi Arabia, Bahrain, Qatar, and the United Arab Emirates*; FAO: Rome, Italy, 1997; Volume VII, pp. 1–293.
64. Yang, C.P.; Li, H.X.; Li, L.; Xu, J.; Yan, Y. Population Structure, Morphometric Analysis and Reproductive Biology of *Portunus Sanguinolentus* (Decapoda: Brachyura: Portunidae) in Honghai Bay, South China Sea. *J. Crustacean Biol.* **2014**, *34*, 722–730. [[CrossRef](#)]
65. Carvalho, F.L.; Carvalho, E.A.S.; Couto, E.C.G. Comparative analysis of the distribution and morphological sexual maturity of *Persephona lichtensteinii* and *P. punctata* (Brachyura, Leucosiidae) in Ilhe'us, BA, Brazil. *Nauplius* **2010**, *18*, 109–115.
66. Signa, G.; Cartes, J.E.; Solé, M.; Serrano, A.; Sánchez, F. Trophic ecology of the swimming crab *Polybius henslowii* Leach, 1820 in Galician and Cantabrian Seas: Influences of natural variability and the Prestige oil spill. *Cont. Shelf Res.* **2008**, *28*, 2659–2667. [[CrossRef](#)]
67. Van Couwelaar, M.; Angel, M.Y.; Madin, L.P. The distribution and biology of the swimming crab *Charybdis smithii* (McLeay, 1938) (Crustacea; Brachyura; Portunidae) in the NW Indian Ocean. *Deep-Sea Res. II* **1997**, *44*, 1251–1280. [[CrossRef](#)]
68. Robinson, C.J.; Anislado, V.; Lopez, A. The pelagic red crab (*Pleuroncodes planipes*) related to active upwelling sites in the California current off the west coast of Baja California. *Deep-Sea Res. II* **2004**, *51*, 753–766. [[CrossRef](#)]
69. Hu, J.; Wang, X.H. Progress on upwelling studies in the China seas. *Rev. Geophys.* **2016**, *54*, 653–673. [[CrossRef](#)]
70. Rome, M.S.; Young-Williams, A.C.; Davis, G.R.; Hines, A.H. Linking temperature and salinity tolerance to winter mortality of Chesapeake Bay blue crabs (*Callinectes sapidus*). *J. Exp. Mar. Biol. Ecol.* **2005**, *319*, 129–145. [[CrossRef](#)]
71. Batoy, C.B.; Sarmago, J.F.; Pilapil, B.C. Breeding season, sexual maturity and fecundity of the blue crab, *Portunus pelagicus* (L.) in selected coastal waters in Leyte and vicinity, Philippines. *Ann. Trop. Res.* **1987**, *9*, 157–177.
72. Campbell, G.R. Size at sexual maturity and occurrence of ovigerous females in three species of commercially exploited portunid crabs in SE Queensland. *Proc. R. Soc. Qld.* **1986**, *97*, 79–87.
73. Carvalho, F.L.; Couto, E.C.G. Environmental variables influencing the *Callinectes* (Crustacea: Brachyura: Portunidae) species distribution in a tropical estuary Cachoeira River (Bahia, Brazil). *J. Mar. Biol. Assoc. UK* **2011**, *91*, 793–800. [[CrossRef](#)]
74. Jan, S.; Wang, J.; Chern, C.S.; Chao, S.Y. Seasonal variation of the circulation in the Taiwan Strait. *J. Mar. Syst.* **2002**, *35*, 249–268. [[CrossRef](#)]
75. Soundarapandian, P.; Varadharajan, D.; Boopathi, A. Reproductive Biology of the Commercially Important Portunid Crab, *Portunus sanguinolentus* (Herbst). *J. Mar. Sci. Res. Dev.* **2013**, *3*, 124.
76. Tseng, H.C.; You, W.L.; Huang, W.; Chung, C.C.; Tsai, A.Y.; Chen, T.Y.; Lan, K.W.; Gong, G.C. Seasonal Variations of Marine Environment and Primary Production in the Taiwan Strait. *Front. Mar. Sci.* **2020**, *7*, 38. [[CrossRef](#)]
77. Maestrini, S.Y.; Graneli, E. Environmental-conditions and ecophysiological mechanisms which led to the 1988 chrysochromulina-polylepis bloom-an hypothesis. *Oceanol. Acta* **1991**, *14*, 397–413.
78. Jan, S.; Tseng, Y.H.; Dietrich, D.E. Sources of water in the Taiwan Strait. *J. Oceanogr.* **2010**, *66*, 211–221. [[CrossRef](#)]

